SYNERGISTIC CORROSION INHIBITION ACTIVITY OF THE *CHICORIUMINTYBUS* EXTRACT AND IODIDE IONS FOR MILD STEEL IN ACIDIC MEDIA

EMAD E. EL-KATORI [a*], *A. S. FOUDA* [b] *AND RAHMA R. MOHAMED* [b]

[a] Department of Chemistry, Faculty of Science, New Valley University, El-Kharja-72511, Egypt.
[b] Department of Chemistry, Faculty of Science, Mansoura University, El-Mansoura-35516, Egypt.

ABSTRACT

Herein, An examination into the corrosion inhibition of mild steel (MS) in 1.0 M HCl by the *Chicoriumintybus* extract as a green inhibitor had been achieved via chemical, electrochemical and morphological measurements. The effect of KI additives on corrosion inhibition efficiency was carried out using a weight loss method. The results reveal that the *Chicoriumintybus* extract inhibited the corrosion reaction by adsorption onto the metal/solution interface. Inhibition efficiency, increased with the *Chicoriumintybus* concentration and synergistically increased with the presence of KI. The addition of iodide ions to the *Chicoriumintybus* extract raises inhibition efficiency of 74 to 99%. Polarization data suggest that the *Chicoriumintybus* extract acts as a mixed inhibition-mechanism. This observation was further corroborated by the fit of experimental adsorption data to the Temkin isotherm. The results were confirmed by AFM, SEM images and ATR-IR for the surface morphology.

Keywords: *Chicoriumintybus* extract; Mild steel; Acid corrosion; Synergistic effect, Surface morphology.

1. INTRODUCTION

Iron and its alloys have been one of the majority wasted metals in support of vehicle parts and constructions due to its high malleability [1]. On the other hand, they have been largely liable to corrosion, mainly in acid media. really, acid solutions have been also widely utilized in industrial applications as well as steel and iron, acid pickling, ore creation, chemical processing & cleaning and oil good acidification. Inhibition by inhibitors has been one of the greatest experiments for metal protection against corrosion constantly in acid media for inhibiting unexpected metal dissolution and acid consuming [2,3]. The inhibitors efficiency has been related to the existence of hetero atoms like S, O or N atoms in applicable molecules, heterocyclic compounds and π- electrons [4–6], such chemical inhibitors can adsorbs onto the metal surface and prohibit the active surface sites, therefore lowering the corrosion rate. The polar functional groups have been often observed at the same time as the reaction center for the adsorption process establishment [7,8]. The identified risky causes of the most of synthetic organic inhibitors in addition to restricted environmental policy has been produced it essential to investigate a cheaper one, non-toxic and green natural products as eco-friendly corrosion inhibitors [9]. These organic compounds have been produced or extracted from aromatic herbs, spices and medicinal plants. A large amount of natural products origin have been biodegradable, harmless and easily existing in adequate amount as well as gathering the structural considerations. A variety of plant parts for example leaves, fruits, seeds and flowers have been extracted and utilized as corrosion inhibitors [10–20]. Gained data presented from these studies have been confirmed that *Chicoriumintybus* extract controlled remarkable abilities to restrain the corrosion reaction. *Chicoriumintybus* extract has been followed Asteraceae family, which has been widely acknowledged for medicinal purposes. *Chicoriumintybus* the main sesquiterpene lactones are lactucin, 8 deoxylactucin, and lactucopicrin. There are found in the roots and the heads of the plant and are considered to be responsible for the bitter taste of chicory. The leaves and roots also contain traces amount of bitter of other sesquiterpene lactones such as guaianolides, lactupin, deoxylactupin, eudesmonolides and guanomanolides. it has been a local plant in Egypt. *Chicoriumintybus* has been a major value health food, the whole plant contains a number of medicinally important compounds such as inulin, esculin, volatile compounds (monoterpenes and sesquiterpenes), coumarins, flavonoids and vitamins [21]. It is used as an anti-inflammatory, digestive, diuretic and helps in treatment of spleen enlargement. The plant is used as liver tonic and as an alternative medicine in treating hepato-toxicity. It is used for local application in the treatment of acne, inflammation of throat, and in diarrhea and vomiting [3,4,22,23].

The plan of this work is to check *Chicoriumintybus* extract action as a green corrosion inhibitor on mild steel in 0.1 M HCl solution using Weight loss method (WL), Open circuit potential (OCP), Potentiodynamic polarization (PP), Electrochemical impedance spectroscopy (EIS) and Electrochemical frequency modulation (EFM) techniques. Also, attenuated total reflection-infrared spectroscopy (ATR-IR), Scanning electron microscopy (SEM) and Atomic force microscopy (AFM) analyses have been utilized in order to confirm the inhibition mode.

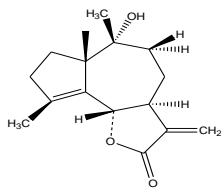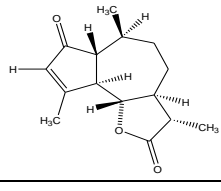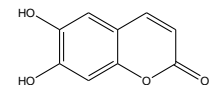## 2. EXPERIMENTAL

2.1 Mild steel (MS) sample

Seven same mild steel samples had been cut out from MS sheets. The listed chemical composition of applicable MS had been (wt%) Fe=99.77, C=0.06495. The MS surface samples and the MS working electrode had been glossed as a mirror finish via various grades (200-2000) from gravel emery papers, cleaned & washed via bi-distilled water and acetone for removing greases. Applicable solution had been 1.0 M HCl, which watery from HCl (37%).

2.2 Chemicals

2.2.1 Plant extract preparation

Chicoriumintybus plant was purchased from the local market and ground into a fine powder to give 200 g of powdered materials which extracted separately by soaking in 70% methanol (300 ml) for 48 h at room temperature. Then the methanolic extract of the sample was concentrated to nearly dryness under reduced pressure by using the rotary evaporator at 45°C to achieve the crude methanolic extract which kept for further investigation.

Table 1. Structure of the main components and formulas and molecular weights of *Chicoriumintybus* extract.

Chicoriumintybus extract	Structure of main components	Formula	Mol. Wt.
1		$C_{16}H_{22}O_3$	262.3
2		$C_{16}H_{20}O_4$	276.3
3		$C_9H_6O_4$	178.1

Corresponding author email: emad.elkatori@scinv.au.edu.eg

The present investigation had been carried out utilizing the plant, namely *Chicoriumintybus.*

The samples had been purchased from the local market and the *Chicoriumintybus* extract stock solution (1000 ppm) had been utilized for preparing the required doses by attenuation via bi-distilled water. *Chicoriumintybus* extract doses range had been between 50 to 300 ppm (D. Mares et al; 2005).

2.2.2 Solutions

a. The applicable solution had been 1.0 M HCl which designed by attenuation of analytical grade HCl (37%) via bi-distilled water. The doses range of the tested green inhibitor had been between 50 to 300 ppm.

b. Potassium iodide solution (KI) had been prepared with 1×10^{-2} M with analytical grade for synergistic effect.

2.3 Measurement techniques

2.3.1 Weight loss method (WL)

WL had been a suitable and widespread procedure to estimate the corrosion inhibitor performance within acid media. The carefully glossed MS samples initial weights had been recorded earlier than inundation into 100 ml of 1.0 M HCl solution in the existence and nonexistence of various *Chicoriumintybus* extract doses which are between 50-300 ppm.

The total inundation time had been 3hr and the experiments have been conducted at various temperatures between 298 and 328 K. Each 30 minutes MS samples had been eliminated from the applicable solution, cleaned & washed with bi-distilled water, after that dehydrated with the air gently and the mass had been calculated again. ML tests had been carried out three times and the average ML had been calculated. Each MS sample's mass had been recorded before and after inundation via 4-Digits laboratory electronic analytical balance.

The (θ) and (IE %) had been computed via the subsequent eq. (1):

$$\% \text{ IE} = \theta \times 100 = [1 - (\Delta W_{inh}/\Delta W_{free})] \times 100 \qquad (1)$$

Where, ΔW_{inh} and ΔW_{free} had been the metal mass losses per unit area in existence and nonexistence of plant extract, correspondingly at a given time period and temperature.

2.3.3 Electrochemical techniques

Electrochemical measurements, involving OCP, PP, EIS and EFM tests had been used. The electrochemical tests had been made via a Gamry three-electrode cell gathering at 25°C. The working electrode (WE) had been MS of 1.0 cm^2, auxiliary electrode had been platinum electrode and reference electrode had been saturated calomel electrode (SCE). The WE had been scraped with various grades of gravel emery papers, cleaned & washed via bi-distilled water and acetone for removing grease after that dried between two filter papers.

All experiments had been achieved for metal samples in 100 ml of 0.1 M HCl in existence and nonexistence of plant extract doses at room temperature. Electrochemical tests had been achieved via Gamry Instrument (PCI4/750) Potentiostat/Galvanostat/ZRA, which involved a Gamry framework system derived from the ESA 400. Gamry applications involve DC105 software for potentiodynamic polarization, EIS 300 software for electrochemical impedance spectroscopy, and EFM 140 software for electrochemical frequency modulation tests using a computer in order to gain data.

2.3.3.1 Open circuit potential (OCP)

In electrochemical experiments, working electrode had been examined like a timer function for the period of 10 minutes. This time requisite to achieve steady state and gained (OCP) value.

2.3.3.2 Potentiodynamic polarization (PP)

Tafel curves had been gained potentiodynamically in a range of - 0.1 to 0.2 V and inspect rate will be 1.0 mVs^{-1}, via the Stern-Geary equation, the linear polarization plot steps had been replaced to obtain corrosion current [24].

The IE % and (θ) had been computed via the subsequent eq. 2:

$$\% \text{ IE} = \theta \times 100 = [1 - (i_{inh} / i_{free})] \times 100 \qquad (2)$$

Where, i_{free} and i_{inh} are the corrosion current densities of uninhibited and inhibited solution, correspondingly.

2.3.3.3 Electrochemical impedance spectroscopy (EIS)

EIS had been conducted via an open-circuit potential (OCP) within the frequency range of (1 Hz to 100 kHz) at an amplitude of 10 mV. Electrochemical functions, for example R_{ct} and C_{dl} values had been obtained and IE % had been computed from charge transfer resistance (R_{ct}) gained from the real (Z') vs. imaginary (Z") plot. The impedance plots had been designed in Nyquist and Bode representation. IE % and (θ) had been obtained from the EIS measurements via the subsequent eq. 3:

$$\% \text{ IE} = \theta \times 100 = [1 - (R°_{ct} / R_{ct})] \times 100 \qquad (3)$$

Where R_{ct} and $R°_{ct}$ are the charge transfer resistance in existence and nonexistence of the applicable extract inhibitor, correspondingly.

2.3.3.4 Electrochemical frequency modulation (EFM)

EFM had been utilized as a novel method to estimate the corrosion rate [25]. EFM tests had been achieved via potential disturbance signal through amplitude of 10 mV through two sine signals of 2 and 5 Hz. The inter-modulation spectra had been included current responses allocated for harmony and inter-modulation current peaks. The higher peaks had been utilized to compute the corrosion current density (i_{corr}), the Tafel slopes (β_a and β_c) and the causality factors CF2 & CF3 [26].

2.4 Surface morphology

2.4.1 Scanning electron microscopy (SEM)

Inspection of MS sample's surface in the existence and nonexistence of the maximum dose of the *Chicoriumintybus* extract (300 ppm) which had been inundated for 24 h at room temperature had been studied via (JEOL JSM-5500, JAPAN) model.

2.4.2 Atomic force microscopy (AFM)

AFM had been a positive tool to contact the fine points of corrosion process at the molecular level. In order to take the surface micrographs, the designed MS samples had been inundated in 1.0 M HCl in the existence and nonexistence of *Chicoriumintybus* extract. After 24 hour the samples were removed from applicable solution, cleaned & washed with bi-distilled water and dried. Thus obtained samples were analyzed by used in a Pico SPM2100 AFM apparatus working in contact mode in air at Nanotechnology Laboratory, Faculty of Engineering, Mansoura University.

2.4.3 Attenuated total reflection-infrared spectroscopy (ATR-IR)

The MS sample's had been inundated in 100 ml of 1.0 M HCl in the existence and nonexistence of 300 ppm of *Chicoriumintybus* extract at room temperature. After 24 h, the sample's had been eliminated and dried by air. Then, the MS sample's surface coating had carefully scratched and the gotten samples utilized to the ATR-IR spectrum test. IR Affinity (Perkin-Elmer) spectrophotometer had been utilized in order to gain ATR-IR data define the composition of the corrosion product obtained on the MS surface.

3. RESULTS AND DISCUSSION

3.1 Weight loss method (WL)

WL-time curves of MS in applicable solution 1.0 M HCl have been determined in the existence and nonexistence of various *Chicoriumintybus* extract doses, which has been shown in Figure 1. The gained corrosion parameters data have been reported in Table 2, from which we have been finding that IE% raises with rising *Chicoriumintybus* extract doses and raises with rising temperature. Lowering in corrosion rate (CR) by rising *Chicoriumintybus* extract doses is as a result of the fact that the metal surface coverage (θ) become larger via the adsorption of inhibitor molecules [27].

The reduce in CR possibly with rising in temperature via the adsorption rate of *Chicoriumintybus* extract on the MS surface has been raised at higher temperatures [28].
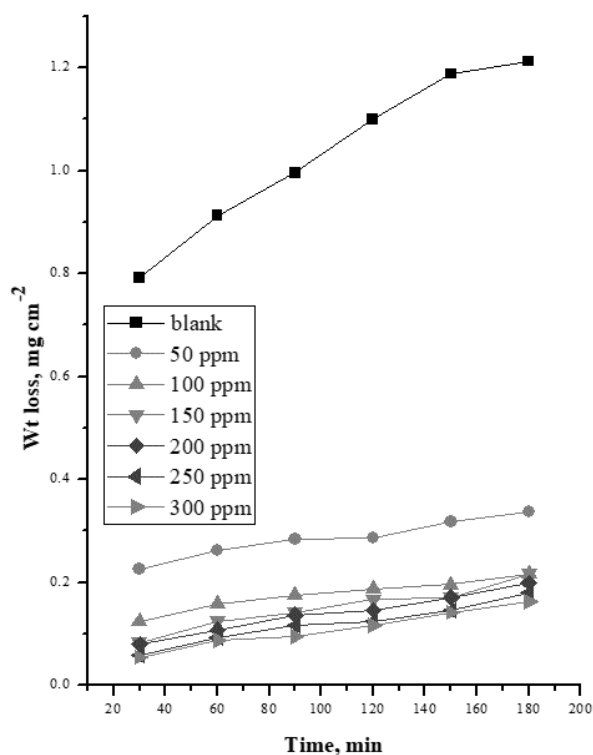

Figure 1. WL *vs.* time plot for corrosion of MS in 1.0 M HCl in the existence and nonexistence of different *Chicoriumintybus* extract doses at 25°C.

Table 2. WL measurements Data for MS in 1.0 M HCl in the existence and nonexistence of different *Chicoriumintybus* extract doses at 25–55°C.

Conc., ppm	Temp., °C	Wt. loss, (mg)	C.R., mg cm⁻²min⁻¹	%IE	Θ
50	25	6.9	0.0020	73.8	0.738
	35	8.7	0.0030	81.6	0.816
	45	8.8	0.0030	83.5	0.835
	55	11.9	0.0040	84.9	0.849
100	25	4.5	0.0020	82.9	0.829
	35	7.6	0.0030	83.9	0.839
	45	7.8	0.0030	85.4	0.854
	55	10	0.0030	87.1	0.871
150	25	4.25	0.0015	83.9	0.839
	35	7.2	0.0025	84.8	0.848
	45	7.1	0.0025	86.7	0.867
	55	8.6	0.0030	89.0	0.890
200	25	3.9	0.0014	85.3	0.853
	35	6.3	0.0022	86.7	0.867
	45	6	0.0021	88.7	0.887
	55	7.8	0.0027	90.0	0.900
250	25	3.25	0.0011	87.7	0.877
	35	5.4	0.0019	88.6	0.886
	45	5.9	0.0020	88.9	0.889
	55	7.5	0.0026	90.4	0.904
300	25	3	0.0010	88.6	0.886
	35	5	0.0017	89.3	0.893
	45	5.7	0.0020	89.4	0.894
	55	6.6	0.0023	91.5	0.915

3.2 Synergistic effect

KI anion is found to enhance the inhibitive effect of the *Chicoriumintybus* extract in acidic solutions [29]. In the present stud, the influence of this anion I^- on the inhibitive performance of the *Chicoriumintybus* extract has been studied using weight loss method.

Figure 2, represent the weight loss-time curves for mild-steel dissolution in 1.0 M HCl for various concentrations of the *Chicoriumintybus* extract and at specific concentration ($1X\,10^{-2}$ M) of this salt. The values of inhibition efficiency (%IE) for various concentrations of inhibitor in the presence of specific concentrations of potassium iodide are given in Table 3.

The synergistic inhibition effect was evaluated using a parameter, S_θ, obtained from the surface coverage values (θ) of the anion, cation and both. Aramaki and Hackerman, calculated the synergism parameter S_θ using the following equation:

$$S_\theta = 1-\theta_{1+2} / 1-\theta'_{1+2} \qquad (3)$$

Where: $\theta_{1+2} = (\theta_1 + \theta_2) - (\theta_1\theta_2)$;

θ_1 = surface coverage by anion;

θ_2 = surface coverage by cation;

θ'_{1+2} = measured surface coverage by both the anion and cation.

We calculate synergism parameters from the above equation. The plot of the synergism parameter (S_θ) against various concentrations of the investigated extract are given in Figure 3 and the corresponding values are shown in Table 3. As can be seen from Table 4 these values nearly equal to unity, which suggests that the enhanced inhibition efficiencies caused by the addition of iodide, to plant extract is due mainly to the synergistic effect.

Finally; It is observed that the inhibition efficiency (%IE) of the inhibitor increases with increasing concentration of inhibitors due to synergistic effects as reported by Cahskan and Bilgic [30]. The synergistic effect of the anions I^- have been observed, this effect depends on the type of anion [31]. Adsorption of the extract at the mild steel/solution interface occurs through chemical adsorption via electron rich centers, i.e. benzene ring through its π-electrons and nitrogen atoms through its lone pair of electrons by donation of electrons to the empty d-orbital of the metal. It is known that I^- anions have strong interactions with mild steel surfaces owing to chemisorption. The strong chemisorption of I^- anions on the metal surface is responsible for the synergistic effect of iodide anions in combination with cation of the inhibitor. The cations are then adsorbed by coulombic attraction on the metal surface where iodide anions are already adsorbed by chemisorption. Stabilization of adsorbed iodide anions with cations leads to greater surface coverage and therefore greater inhibition. From the previous results, it is known that KI could be considered as one of the effective anions for synergistic action within the investigated inhibitor.
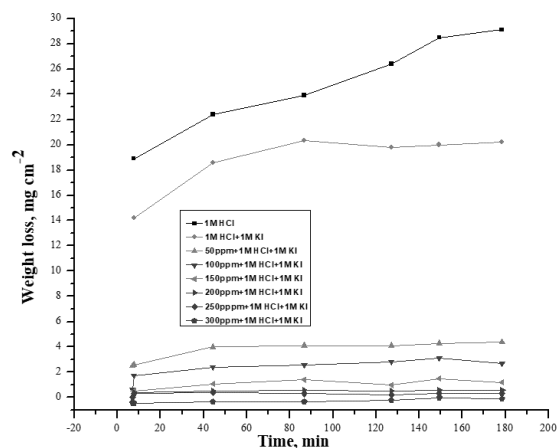

Figure 2. Weight loss-time curve for mild steel dissolution in 1.0 M HCl in the existence and nonexistence of $1x10^{-2}$ M KI in the presence of different concentrations of *Chicoriumintybus* extract at 25°C.
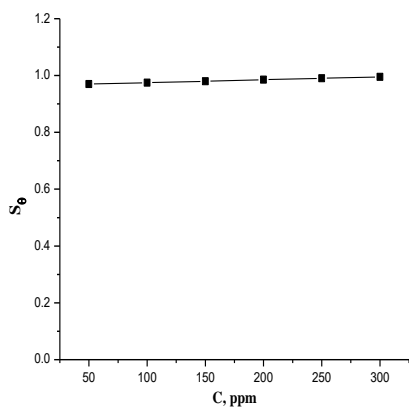
Figure 3. plot of synergism parameter S_θ *vs.* the concentration of *Chicoriumintybus* extract in absence and presence of 1×10^{-2} M KI at 25°C.

Table 3. Inhibition efficiencies Values (%IE) of different concentrations of *chicoriumintybus* extract in the presence of 1×10^{-2} M KI for the corrosion of mild steel in 1.0 M HCl at 25°C.

Conc., ppm	Inhibition efficiency (%IE)	
	Chicoriumintybus	*Chicoriumintybus with KI*
50	73.8	84.4
100	82.9	95.8
150	83.9	97.3
200	85.3	98.1
250	87.7	99.2
300	88.6	99.6

Table 4. Synergism parameter (S_θ) for various concentrations of *chicoriumintybus* extract in the presence of 1×10^{-2} M KI.

Conc., ppm	Synergism parameter (S_θ)
	Chicoriumintybus
50	0.970
100	0.975
150	0.980
200	0.985
250	0.990
300	0.995

3.3. Electrochemical techniques

3.3.1 Open circuit potential (OCP)

Figure 4, has been the indication of the influence of different concentrations of *Chicoriumintybus* extract on the E_{OC} variety of mild steel with time in 1.0 M HCl solution at 25°C. Steady-state data of the E_{OC} are larger negative than the inundation potential (E_{OC} at t=0), indicating so as previous to the steady state condition has been achieved the pre-inundation, air oxide film formed has to break up [32]. This steady state potential ($E_{corr.}$) rapidly obtained (later than 10 min of inundation), be in contact to the bare metal free corrosion [33]. It has been noticeable that ($E_{corr.}$) shifts to larger negative data without the alteration general feature of E/t plot. On the other hand upon rising the concentration of *Chicoriumintybus* extract.
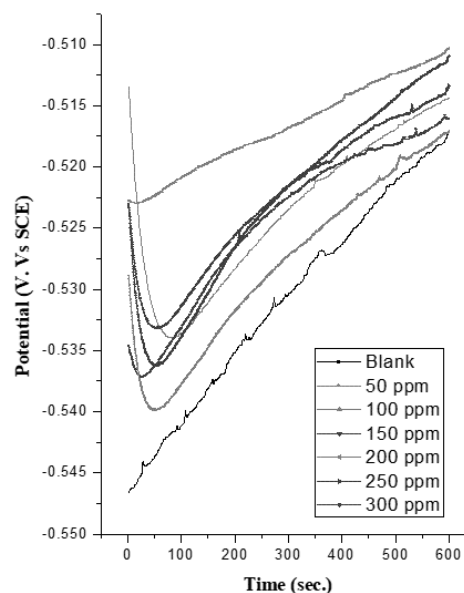

Figure 4. Variation of open circuit potential (E_{OC}) as a parameter of time record for mild steel in 1.0 M HCl in the existence and non existence of different *Chicoriumintybus* extract doses at 25°C.

Firstly, the E_{OC} has been proceeded to lower negative data, achieving a maximum one. After assuring time relying on the *Chicoriumintybus* extract doses, the potential decrease and arrive a reasonably steady value. These data have been elucidated that two counter-appearing processes happened, the initial one has been a creation of protective adsorbed film on the electrode surface, in addition to a result delayed-action corrosion takes place which moving E_{OC} values towards more noble data. Corrosion has been occurring on the next one, which has been made potential back towards among these two counter performing operations can possibly elucidate semblance of an arrest or peak in E_{OC} vs. time plot as presented in Figure 4. The steady-state potential proceed towards larger negative data with rising the *Chicoriumintybus* extract doses. Initially, E_{OC} has been shifted to lower negative values (as a result of corrosion inhibition) accomplishing high one. In addition to, after a suitable time the potential has been reduced to achieve a reasonably steady value (as a result of metal dissolution), which effect the corrosion potential steady state proceeding towards larger negative value. These data illuminate that the *Chicoriumintybus* extract is an efficiency corrosion inhibitor.

3.3.2 Potentiodynamic polarization (PP)

PP measurements have been applied to discuss the influence of *Chicoriumintybus* extract on both anodic and cathodic processes occurring in the system. From Table 5, It has been clear that i_{corr} data are reducing with rising inhibitor doses, which obviously illustrates corrosion inhibition IE%. From Figure 5, it has been obvious that *Chicoriumintybus* extract delay both anodic and cathodic processes, and also supported by the gained data in Table 3. Both β_a and β_c data have been changed, in other hand, there has been no normal displacement pattern in E_{corr} data which have been illustrated that *Chicoriumintybus* extract act as a mixed type inhibitor. Via Ferreira and others [34], if the corrosion potential displacement has been larger than 85 mV relating to the corrosion potential of blank, *Chicoriumintybus* extract may be act as anodic or cathodic type.
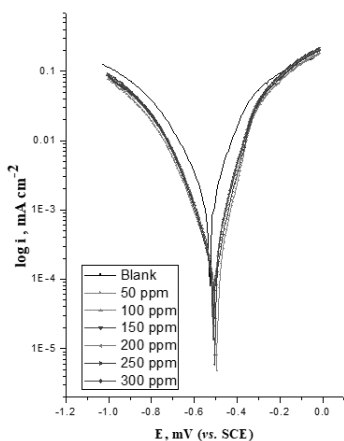
Table 5. PP values of MS in 1.0 M HCl in existence and nonexistence of different *Chicoriumintybus* extract doses at 25°C.

Conc., ppm	- E_{corr}, mV vs SCE	i_{corr}, µA cm^{-2}	β_c mV dec^{-1}	β_a mV dec^{-1}	C.R, mpy	IE%	Θ
Blank	528	1460	169	74	8.6	-----	------
50	509	284	142	91	129.8	80.5	0.805
100	511	248	137	92	113.5	83.0	0.830
150	511	244	131	87	111.3	83.3	0.833
200	510	239	133	89	109.3	83.6	0.836
250	506	183	130	85	83.8	87.5	0.875
300	496	147	132	77	67.0	89.9	0.899

Figure 5. PP curves of the corrosion of MS in 1.0 M HCl in the existence and nonexistence of different *Chicoriumintybus extract* doses at 25°C.

3.3.3 Electrochemical impedance spectroscopy (EIS)

EIS has been an embedded and influential tool in corrosion measurements. The electrochemical process happening at the OCP has been studied via EIS to facilitate gaining a mechanistic conception, electrode kinetics, MS surface properties of corrosion in the existence of *Chicoriumintybus* extract [35]. Figure 6, has been illustrated Nyquist plots, which included a semicircle; the diameter has been larger by rising the *Chicoriumintybus* extract doses. This has been denoted that inhibition efficiency is directly proportional to the *Chicoriumintybus* extract doses. The capacitive loop shapes have been shown that the corrosion process has been largely charge transfer restriction [36]. The rising in charge transfer resistance (R_{ct}) via *Chicoriumintybus* extract doses denotes significant inhibitor surface coverage and surface strong bonding. The Nyquist plots have been evaluated by way of the equivalent circuit shown in Figure 7, which has been commonly utilized in order to explain given EIS data. The R_{ct} data have been raised and double layer capacitance (C_{dl}) data lowered with rising in *Chicoriumintybus* extract doses, which has been most likely via lowering the local dielectric constant or rising electrical double layer thickness. This recommends that *Chicoriumintybus* extract strongly adsorbed on the MS surface [37]. Rising in R_{ct} data and lowering in the C_{dl} data causes an increase in the inhibition efficiency IE%. Data have been gained for MS in 1.0 M HCl solution in the existence and nonexistence of different *Chicoriumintybus* extract doses. while Nyquist plots data gained for the inhibitor present, which are exhibiting a circle, such manner has been attributed for solid electrodes and is commonly shared to a frequency dispersion creating from the surface irregularity. The C_{dl} data have been gained from subsequent eq. 4:

$$C_{dl} = 1 / 2\pi R_{ct} f_{max} \qquad (4)$$

Where, f_{max} symbolizes the frequency at which imaginary data arrives a maximum at Nyquist plots. In Bode plots which are shown in Figure 6, the larger frequency border refers to the solution resistance R_S (Ω), however the minimum frequency border refers to ($R_{ct} + R_s$). The lower frequency illustrates the charge transfer reaction kinetic response [38]. The corrosion parameters of impedance tests have been shown in Table 6. The gained data have been illustrated that R_{ct} values raises with rising the *Chicoriumintybus* extract doses, which drives to IE% have been increased and double layer capacitance (C_{dl}) data have been reduced in the existence of the inhibitor.

The lowering in C_{dl} due to a reduce in local dielectric constant and/or arising in double layer thickness. therefore, it has been reasonable to reduce functions presented in inhibitor extract via the metal- acid interface adsorption [39]. It is clear that there has been a good congruence between the two dissimilar electrochemical measurements, due to that the same trend of inhibition of the *Chicoriumintybus* extract.
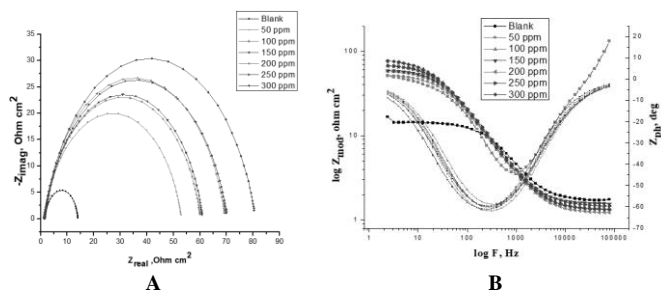

| A | B |

Figure 6. The Nyquist (a) and Bode (b) curves for the corrosion of MS in 1.0 M HCl in the existence and nonexistence of different *Chicoriumintybus* extract doses at 25°C.
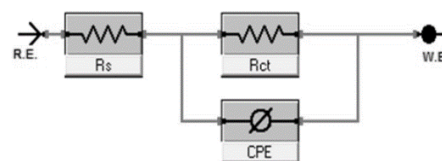

Figure 7. Equivalent circuit as a model for impedance data for MS in 1.0 M HCl solution.

Table 6. EIS parameters for corrosion of MS in 1.0 M HCl in the existence and nonexistence of the different *Chicoriumintybus* extract doses at 25°C**.**

Conc., ppm	R_{ct}, Ω cm²	C_{dl}, μFcm⁻²	IE%	θ
Blank	12.3	47	----	----
50	51.8	38	76.2	0.762
100	58.9	35	79.1	0.791
150	59.5	32	79.3	0.793
200	68.4	29	82.0	0.820
250	68.8	25	82.1	0.821
300	79.6	20	84.5	0.845

3.3.4 Electrochemical frequency modulation (EFM).

The current-frequency spectral chart gained from EFM tests in the existence and nonexistence of different *Chicoriumintybus* extract doses have been illustrated in Figure 8. The spectra have been analyzed to calculate i_{corr}, β_a, β_c and the causality factors (CF-2 and CF-3) which have been reported in Table 7. From this Table We noticed that i_{corr} has been reduced with rising *Chicoriumintybus* extract doses and the IE% has been raised via rising the extract doses. The change in magnitudes of β_a and β_c values was also small, indicating that the existence of extract doesn't adjust the corrosion mechanism. The causality factors CF-2 and CF-3 which have been gained are closed to theoretical values of 2 and 3 correspondingly, showing that the gained values have been verified and good quality [40].
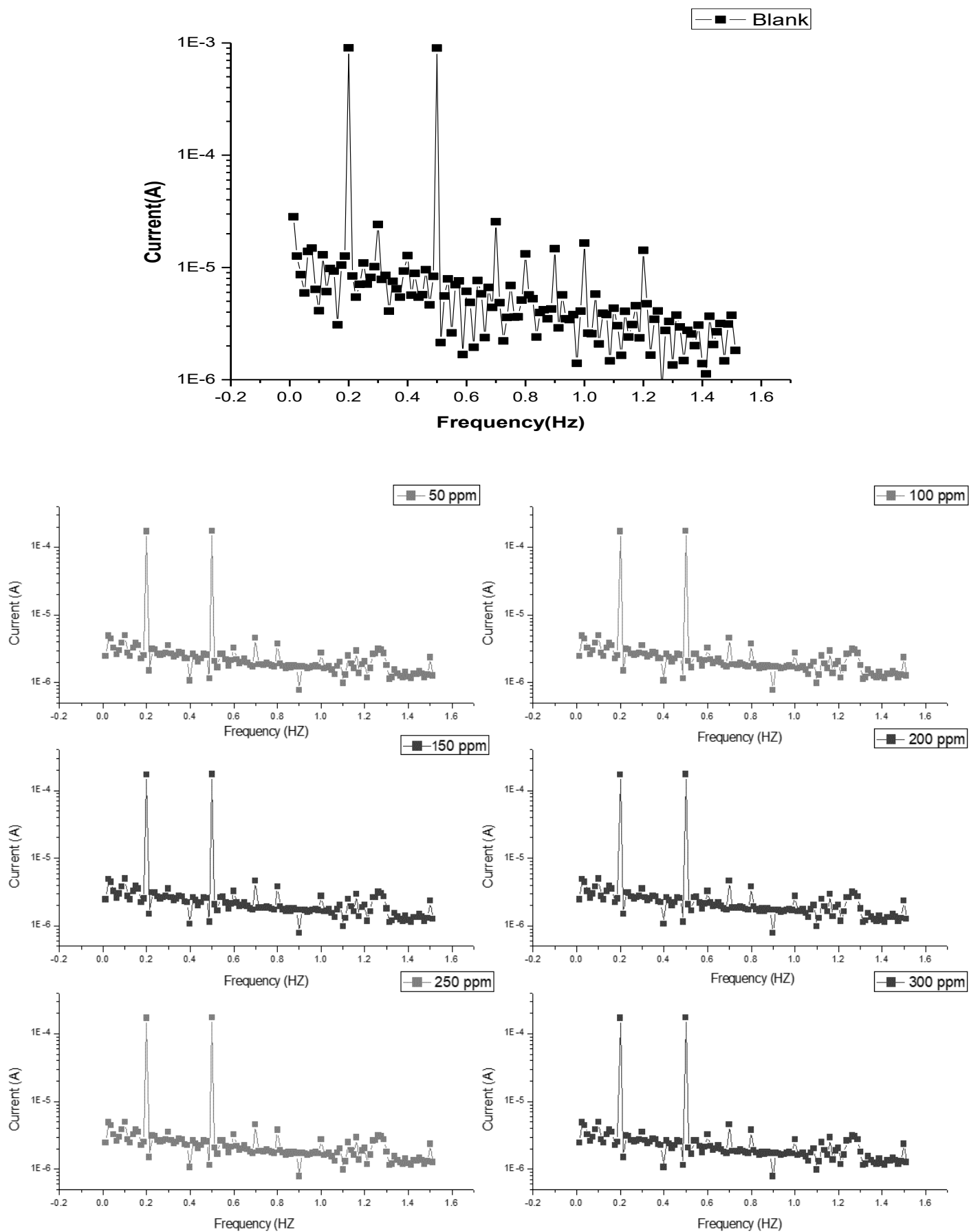
Table 7. Electrochemical kinetic parameters gained via EFM test for MS in 1.0 M HCl in the existence and nonexistence of the different *Chicoriumintybus* extract doses at 25°C.

Conc., pm	i_{corr}, μAcm⁻²	β_c, mVdec⁻¹	β_a, mVdec⁻¹	CF-2	CF-3	C.R, mpy	IE%	θ
Blank	528	1460	169	74	8.6	-----	------	Blank
50	304	98	93	1.9	2.8	139.0	78.6	0.786
100	295	100	92	1.9	3.2	135.0	79.2	0.792
150	274	106	89	1.9	3.1	125.3	80.8	0.808
200	254	98	83	1.9	2.8	116.2	82.2	0.822
250	235	95	95	1.9	2.7	107.5	83.5	0.835
300	216	106	85	1.9	2.8	98.6	84.8	0.848

Figure 8. Inter-modulation spectrum for the corrosion of MS in 1.0 M HCl in the existence and nonexistence of different *Chicoriumintybus* extract doses at 25ºC.

3.4 Adsorption isotherms

Corrosion inhibitors influence is reliant on MS surface adsorption modes. while the interaction forces between MS surface and water molecules has been minor than another one between the MS surface and the inhibitor compound, a replacement adsorption process may be created and water molecules adsorbed on the MS surface, $(H_2O)_{ads}$ molecules have been substituted by inhibitor molecules in the aqueous phase ($inhibitor_{aq}$).

$$xH_2O_{ads} + Inhibitor_{sol} \leftrightarrow Inhibitor_{ads} + xH_2O \qquad (5)$$
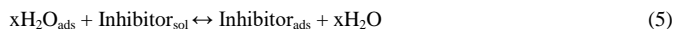
Where x characterizes the size ratio, the number of water molecules replaced with one inhibitor molecule. The inhibitor adsorption process may either happen physically or chemically on a corroded MS surface, wherever the physisorbed molecules delay metal dissolution by blocking the cathodic reaction, even as chemisorbed molecules block the anodic reaction via lowering the ingrained reactivity on the metal adsorption sites.

Essential knowledge on the interaction between metal surface & plant extract has been supplied via the adsorption isotherms [41]. Therefore, in order to collect most knowledge about the adsorption mode of *Chicoriumintybus* extract on the MS surface in 1.0 M HCl at various temperatures. Efforts have been prepared to fit experimental data by a number of adsorption isotherms as Langmuir, Temkin, Freundlich, Bockris−Swinkles and Flory−Huggins isotherms. On the other hand, the top fit has been resulted via Temkin isotherm, which has been in a good agreement with subsequent eq. (6):

$$InK_{ads}C = a\theta \qquad (6)$$

Where K_{ads}, the adsorption reaction equilibrium constant, C, the inhibitor concentration in the bulk of solution, (a) the interaction parameter and (θ) the surface coverage.

Plots of θ vs. log C for plant additives adsorption on the MS surface in 1.0 M HCl acid at 25- 55°C has been illustrated in Figure 9. The gained results create straight lines demonstrating that Temkin's isotherm has been available for applied systems.

($\Delta G°_{ads}$) was calculated from subsequent eq. (7):

$$\Delta G°_{ads} = -RT \ln 55.5 K_{ads} \qquad (7)$$

Where R is the gas constant and T is the absolute temperature. 55.5 value has been the water concentration in solution in mol l^{-1}. To calculate heat of adsorption ($\Delta H°_{ads}$), a plot of log $\Delta G°_{ads}$ vs. T was done Figure 10. The intercept would be equal to $\Delta H°_{ads}$ according to the subsequent equation:

$$\Delta G°_{ads} = \Delta H°_{ads} - T \Delta S°_{ads} \qquad (8)$$

The adsorption entropy ($\Delta S°_{ads}$), could be calculated from the previous equation and the data of (K_{ads}), ($\Delta G°_{ads}$), ($\Delta H°_{ads}$) and ($\Delta S°_{ads}$) are reported in Table 8. These data indicate that:

The adsorption entropy ($\Delta S°_{ads}$), which obtained via the subsequent equation:

$$\Delta G°_{ads} = \Delta H°_{ads} - T \Delta S°_{ads} \qquad (9)$$

The data of (K_{ads}), ($\Delta G°_{ads}$), ($\Delta H°_{ads}$) and ($\Delta S°_{ads}$) are reported in Table 8. These data indicate that:

i. The values of K_{ads} increase with rising in temperature. The detected reports indicated that K_{ads} obtained from the Temkin isotherm has been raised with temperature rising.
ii. $\Delta G°_{ads}$ have a negative sign, be a sign of the extract is spontaneously adsorbed on the metal surface [42].
iii. $\Delta G°_{ads}$ values has been found around -40 kJ mol^{-1} referring that the adsorption nature for *Chicoriumintybus* extract in 1.0 M HCl has been chemical adsorption [43].
iv. $\Delta H°_{ads}$ a positive sign, refer to that the extract adsorption process has been an endothermic process [44].
v. $\Delta S°_{ads}$ have positive values, has been frequently characteristic to endothermic adsorption process.

Generally, an endothermic process has been typically characteristic to chemisorption via electron transfer from inhibitor to metal surface in order to create co-ordination bond while exothermic adsorption process suggests either physisorption or chemisorption [42]. The lone pairs of electrons in estimated molecules can be interacted with vacant MS d-orbital in order to create chemisorbed film.
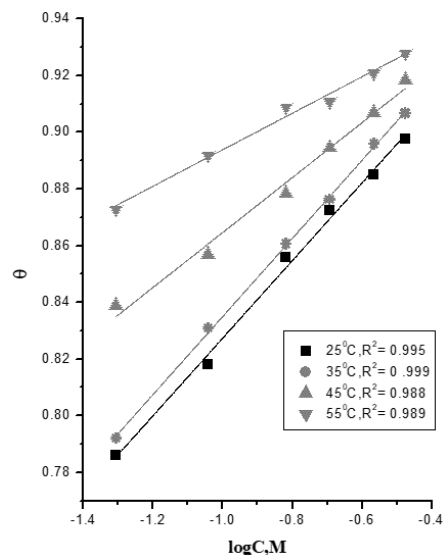

Figure 9. Temkin adsorption curves for MS in 1.0 M HCl with different *Chicoriumintybus* extract doses at different temperatures.

Table 8. Adsorption thermodynamic functions of the *Chicoriumintybus* extract on MS surface in 1.0 M HCl at different temperatures.

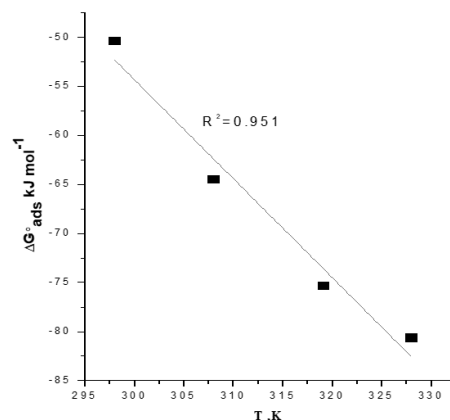| Temp., °C	log K_{ads}, M^{-1}	-$\Delta G°_{ads}$ kJ mol^{-1}	$\Delta H°_{ads}$ kJ mol^{-1}	$\Delta S°_{ads}$ J mol^{-1}K^{-1}
25	7.1	50.5		233.6
35	9.2	64.5	19.1	271.7
45	11	77.6		304.2
55	11.1	80.6		304.3

Figure 10. $\Delta G°_{ads}$ has been plotted *vs.* T(K) for the *Chicoriumintybus* extract.

3.5 Kinetic-thermodynamic corrosion parameters

Usually, chemisorption process has been a sign of the higher value of E_a detected for free acid solution match up to the inhibited one. This may be clarified that the total corrosion process shift from exposed surface to adsorbed sites accounts for E_a reducing at larger inhibition levels [45]. as well, lowering E_a at higher temperatures may be correlated with rising inhibitor molecules adsorption onto the metal surface.

Table 9 illustrated that the E_a data on the existence of the *Chicoriumintybus* extract are less than the blank solution one, which assists chemisorption process wherein the co-ordination bond has been created via inhibitor participation and/or electrons transition to MS surface atoms involving vacant-d-orbital, so the anodic reaction of the corrosion process take place [46].

On the other hand, a low E_a value in the existence of inhibitor molecules matches up to free solution has been recommended chemisorption process of inhibitor molecules. The E_a^* values listed in Table 9 have been comparatively close and follow the same pattern, which agree with the transition-state theory model. Enthalpy of activation ΔH^* has a positive value, which has been signified that the metal dissolution process has been endothermic [47]. This also has been achieved to be investigated of delayed metal corrosion in inhibitor containing solution.

The *Chicoriumintybus* extract Entropy values (ΔS^*) have been negative, referring that the rate determining step been included association further than the dissociating phenomenon of activated complex creation [48]. From which, transition process from reactants to activated complex has been followed by lowering in a mess. In the inhibitors existence, the hydrogen ion discharge to create adsorbed hydrogen atoms at the metal surface can be blocked via the inhibitor molecule adsorption. This reasons allows the system to exceed further orderly to a less orderly arrangement.

The apparent activation energy (E_a^*), the activation enthalpy (ΔH^*) and the activation entropy (ΔS^*) for the dissolution of MS samples in 1.0 M HCl solution in the existence and nonexistence of different *Chicoriumintybus* extract doses have been computed via Arrhenius and transition-state eqns. (10 &11):

$$\text{Rate } (k_{corr}) = A \exp(-E_a^*/RT) \tag{10}$$

$$\text{Rate } (k_{corr}) = RT/Nh \exp(\Delta S^*/R) \exp(-\Delta H^*/RT) \tag{11}$$

Where, A is the Arrhenius pre-exponential factor, h is the Plank's constant and N is Avogadro's number. Figure 11 represents, plot of log k_{corr} *vs.* 1/T in 1.0 M HCl of different extract doses, as of the slope in Figure 11, the E_a^* data have been computed. Figure 12 illustrates a plot of log k_{corr}/T *vs.* 1/T gives a straight line its slope of $\Delta H/2.303R$ and intercepts of log R/Nh + $\Delta S^*/2.303$. E_a^* data of the inhibited solutions have been lower than that of uninhibited ones referring that the MS corrosion has been reduced via the creation of the inhibitor adsorption protective film on the MS surface. The calculated data of (E_a^*), (ΔH^*) and (ΔS^*) have been recorded in Table 9, which inform that:

i. The existence of examining extract reducing the E_a^* and consequently reducing the CR (k_{corr}) of MS via forming a barrier to mass and charge transfer and by their adsorption on the MS surface.
ii. ΔH^* positive signs be a sign of the endothermic nature of the MS dissolution process [49].
iii. The values of ΔS^* in existence and nonexistence of examining extract has been negative, which refers to the activated complex in the rate-determining step characterizes an association rather than dissociation [50,51], which refer to the activated molecules have been in a less-order state than that at the initial state.
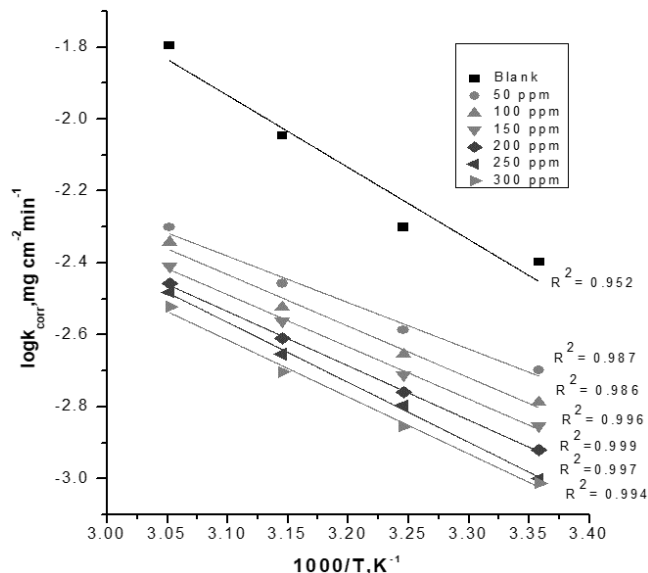

Figure 11. Arrhenius curves for MS corrosion in 1.0 M HCl in the existence and non existence of the different *Chicoriumintybus* extract doses.
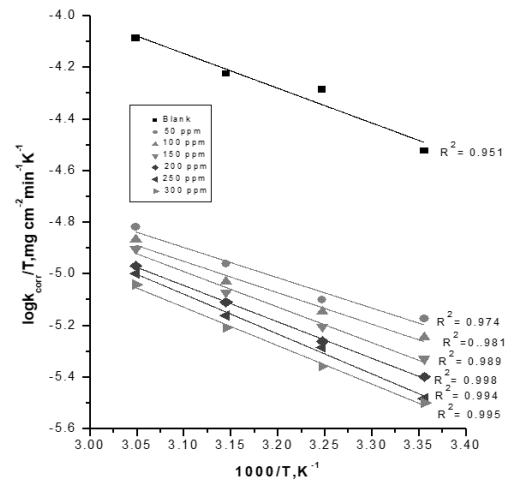

Figure 12. Transition-state for MS corrosion (log k_{corr}/T) in 1.0 M HCl in the existence and nonexistence of the different *Chicoriumintybus* extract doses.

Table 9. Activation parameters for MS in the existence and nonexistence of the different *Chicoriumintybus* extract doses in 1.0 M HCl.

Conc., ppm	E_a^*, kJ mol^{-1}	ΔH^*, kJ mol^{-1}	$-\Delta S^*$, J mol^{-1}K^{-1}
Blank	38.3	16.6	-274.7
50	30.6	15.8	-289.5
100	29.6	14.1	-290.2
150	26.8	13.3	-291.1
200	25.8	12.5	-291.7
250	24.8	11.6	-292.9
300	23.9	10.8	-293.3

3.6 Surface analysis

3.6.1 Scanning electron microscopy (SEM)

The MS surface examination via SEM instrument. Figures13[a-c] of the MS surface in 1.0 M HCl solution exhibits the transforms which happened through the corrosion process in the existence and nonexistence of the *Chicoriumintybus* extract. Figure 13$_a$ has been illustrated SEM image of polished MS with comparatively smooth surface, MS surface after inundation in 1.0 M HCl solution has been drastically damaged Figure 13$_b$, in the existence of 300 ppm of the *Chicoriumintybus* extract, surface has been remarkably advanced Figure 13$_c$. This advance in surface morphology is a sign of the protecting layer creation of the *Chicoriumintybus* extract on the MS surface that one is responsible for inhibition and reduction in the corrosion rate [52].
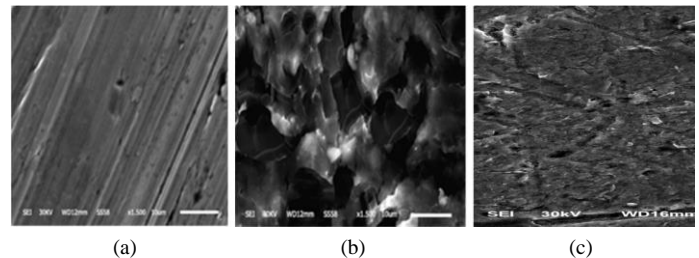

Figure 13. SEM images of MS surface (a) before of inundation in 1.0 M HCl, (b) after 24 h of inundation in 1.0 M HCl and (c) after 24 h of inundation in 1.0 M HCl + 300 ppm of the *Chicoriumintybus* extract at 25ºC.

3.6.2 Atomic force microscopy (AFM)

AFM has been a significant tool in order to estimate the surface morphology investigation that one have been helpful to discuss the inhibitor effect on the metal/solution interface [53]. Figures14[a-c], illustrated the AFM graphs of polished MS, MS in 1.0 M HCl, which not including the *Chicoriumintybus* extract and MS in 1.0 M HCl containing 300 ppm of the *Chicoriumintybus* extract, respectively. From AFM micrographs, the surface is very obvious for

polished MS samples with average roughness 33.4 nm as shown in Figure 14$_a$. Whereas in the nonexistence of the *Chicoriumintybus* extract, the MS surface has been more corroded, with average roughness 667.5 nm as shown in Figure 14$_b$. By comparison, the average roughness have been reduced to 147 nm in the existence of the *Chicoriumintybus* extract at the optimum dose (300 ppm) as shown in Figure 14$_c$. From the results, we concluded that the lowering in the roughness can be very well understand to be via the adsorbed protecting layer creation of the *Chicoriumintybus* extract on the MS surface.
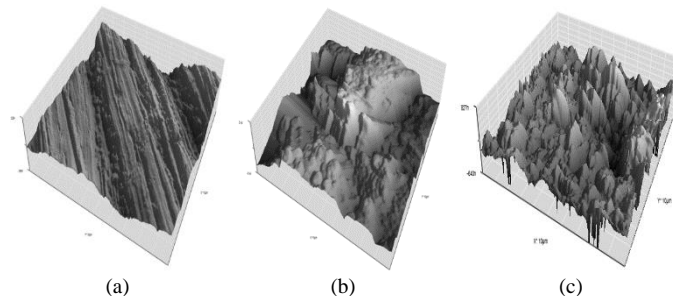

(a)   (b)   (c)

Figure 14. AEM images of MS surface (a) before of inundation in 1.0 M HCl, (b) after 24 h of inundation in 1.0 M HCl and (c) after 24 h of inundation in 1.0 M HCl + 300 ppm of *Chicoriumintybus* extract at 25ºC.

3.6.3 Attenuated total reflection-infrared spectroscopy (ATR-IR)

ATR-IR displays interesting features such as a high signal to noise ratio, high sensitivity and selectivity, accuracy, mechanical simplicity, short analysis time and small amount of sample required for the analysis. Figure 15 shows the ATR-IR spectra of the *Chicoriumintybus* extract. The broad band obtained at 3335 cm^{-1} can be assigned to (O-H), the one at 1643 cm^{-1} corresponds to (C=C), the -C=C stretching frequency appears at 1455 cm^{-1}, the band at 1378 cm^{-1} can be assigned to aromatic nitro compound stretching ,the sharp one at band at 1085 cm^{-1} corresponds to (C-O) stretch, the frequency at 1046 cm^{-1} is due to (=CH$_2$, =C-H), the Nitrate NO$_2$ bending frequency at 721 cm^{-1}.

By comparing the spectra of the extract with that of the solid corrosion product shown in Figure 15, it is observed that there are shifts in the frequencies. It was found that (O-H) stretch at 3335 cm-1 was shifted to 3332 cm^{-1}, the -C=C stretch at 1455cm^{-1} was shifted to 1472 cm^{-1},the aromatic nitro compound at 1378 cm^{-1} has disappeared ,the (C-O) stretch at 1085 cm^{-1} was shifted to 1010 cm^{-1}, the (=CH$_2$, =C-H) stretch at 1046 cm-1 was shifted to 950 cm^{-1}, the Nitrate No$_2$ bending frequency at 721 cm^{-1} has disappeared. The shifts in the spectra indicate that the interaction between the extract and mild steel that occurred through the functional groups found in it [54].

This study has been recommended that the *Chicoriumintybus* extract has been coordinated with Fe^{2+}, through the oxygen atom of the hydroxyl groups, resulting in the Fe^{2+} – inhibitor complex creation on the metal surface anodic sites [55]. Thus, the ATR-IR spectral study shows the creation of the adsorbed layer consists of Fe^{2+}– inhibitor complex via chemisorptions process.
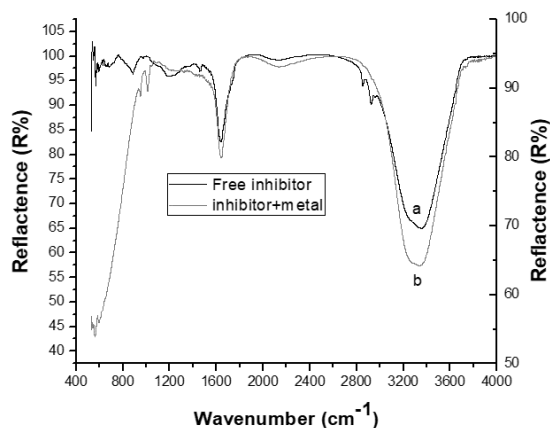

Figure 15. ATR-IR spectroscopy of (a) *Chicoriumintybus* extract and (b) the film formed on the MS surface after inundation in 1.0 M HCl + 300 ppm of *Chicoriumintybus* extract for 24 h at 25ºC.

3.7 Mechanism of corrosion inhibition

The extract adsorption may be explained via two main processes of interactions: physisorption and chemisorptions. Generally, physisorption needs the existence of both charged species in solution and metal surface which electrically charged. The metal surface charge of the electric field presented in the metal/solution interface. In contrast, a chemisorption process may include charge transfer or charge sharing from the inhibitor molecules to the metal surface to form a coordination bond. This has been achieved in the case of a positive as well as a negative charge on the metal surface. The transition metal existence in which involving vacant, low-energy electron orbital's (Fe^{2+} and Fe^{3+}) and the *Chicoriumintybus* extract molecules which having bound electrons or heteroatom's involving a lone pair of electrons have been essential for the large inhibiting action [56]. Commonly, there have been two kinds of inhibition mechanisms have been suggested. One has been the creation of polymeric complexes with iron ions (Fe^{3+}) relying on the applied conditions [57], the other one has been the chemical adsorption of the *Chicoriumintybus* extract on the MS surface [58]. The inhibition achievement of the *Chicoriumintybus* extract doses hasn't been happened via the simple blocking at the MS surface, chiefly at high temperature. This could be referred to the dissimilar adsorption capacities of the *Chicoriumintybus* extract on the MS surface at different temperatures. We have been discussing that while rising temperature the *Chicoriumintybus* extract adsorption effect on MS surface raised. Most of the hydrophilic groups which have positively charged atoms (O$^+$) adsorbed from the MS surface and influence to allow the H$^+$ became closer to the metal surface. As a result, the *Chicoriumintybus* extract has been preferred blocking both anodic and cathodic corrosion processes at higher temperatures as shown in Figure 16.
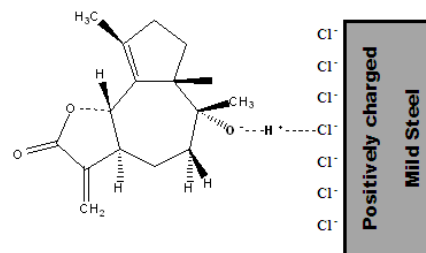

Figure 16. Possible adsorption process of protonated compound from *Chicoriumintybus* extract on mild steel surface in 1.0 M HCl.

4. CONCLUSION

The inhibition efficiency IE% raises by rising the *Chicoriumintybus* extract doses and increases as the temperature rising as illustrated in Figure 17. Adsorption of the *Chicoriumintybus* extract molecules on the MS surface is found to obey Temkin adsorption isotherm model. Polarization curves referred that the *Chicoriumintybus* extract acted as a mixed type inhibitor. ATR-IR spectrum approved that the extract adsorbed on the metal surface. ATR-IR, SEM and AFM images indicated the possibility of creation of the protecting layer on the MS surface. Derived from all results of ML, PP, EIS and EFM, the *Chicoriumintybus* extract had been shown as an effective inhibitor for MS in 1.0 M HCl.
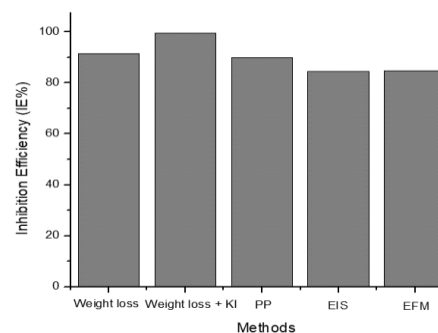

Figure 17. Comparison of inhibition efficiency (IE%) resulted from experimental methods for corrosion of MS in 1.0 M HCl containing 300 ppm of *Chicoriumintybus* in addition to (IE%) resulted from (300 ppm of *Chicoriumintybus*+ 1 ml KI) at 25°C.

REFERENCES

1. N. K. Bakirhan, A. Asan, N. Colak, S. Sanli, J Chil Chem Soc 61, 3066, (2016).
2. Evrim Baran, Ahmet Cakir, BirgülYazici Arab. J. Chem 3, 1, (2016).
3. Noha Fathalla, Mokhtar Bishr, Abdel-Nasser Singab, and Osama Salama, IOSR-JPBS 10, 70, (2015).
4. N. Lebe, N. Geoerge, N. Justus, E. Nneka, and E. peter, Int J Mat Chem 6, 2, (2016).
5. A. Yildirim and M. Cetin, Corros Sci 5, 155, (2008).
6. Abd El-Aziz S. Fouda, Ayman Y. El-Khateeb, Nabila M. Elbahrawi, Zastita Materijala 58, 131, (2017).
7. H. H. Karim, A. K. Anees and H. K. Noor, SAJCE 22, 1, (2016).
8. L. G. Da Trindade and R. S. Goncalves, Corros Sci 51, 1578, (2009).
9. Marko Chigondo and Fidelis chigondo, J Chem 2016, 7 pages, (2016).
10. Saviour A. Umoren, Moses M. Solomon, Ime B. Obot, & Rami K. Suleiman, J Adhes Sci Technol 17, 1934, (2018).
11. S. A. Umoren, I. B. Obot, Z. M. Gasem, Ionics 21, 1171, (2015).
12. N. Soltani and M. Khayatkashani, Int J Electrochem Sci 10, 46, (2015).
13. K. K. Anupama, K. Ramya, and A. Joseph, Measurement 95, 297, (2017).
14. M. H. Hazwan, M. J. Kassim, N. N. Razali, N. H. Dahon and D. Nasshorudin, Arab J Chem 9, S616, (2016).
15. T. H. Ibrahim, E. E. Gomes, I. B. Obot, M. Khamis, and M. A. Sabri, J Adhes Sci Technol 31, 2697, (2017).
16. S. Perumal, S. Muthumanickam, A. Elangovan, R. Karthik, and K. K. Mothilal, J Bio Tribo-Corr 3, 1, (2017).
17. E. B. Ituen, A. O. James and O. Akaranta, JMES 8, 1498, (2017).
18. L. L. Liao, S. Mo, H. Q. Luo, and N. B. Li, J Colloid Interf Sci 499, 110, (2017).
19. E. Ituen, O. Akaranta, A. James and S. Sun, J SM&T 11, 12, (2017).
20. H. L. Y. Sin, A. A. Rahim, C. Y. Gan, B. Saad, M. I. Salleh and M. Umeda, Measurement 109, 334, (2017).
21. S. Nandagopal and B. D. Ranjitha Kumari, Adv Biol Res 1, 17, (2007).
22. R. Kumari, M. Ali, and V. Aeri, J Asian Nat Prod Res 14, 7, (2012).
23. Heibatollah, S. Reza, Nikbakht Mohammad; Izadpanah Ghaitasi, Sohailla Sabzali, Afr J Biochem Res 2, 141, (2008).
24. R. Baskar, D. Kesavan, M. Gopiraman, Prog Org Coat 77, 836, (2014).
25. M. A. Migahed, E. G. Zaki, M. M. Shaban, RSC Adv 6, 71384, (2016).
26. K. K. Anupama, K. Ramya and A. Joseph, Measurement 95, 297, (2017).
27. Abd El-Aziz Fouda, Ahmed Al-Sarawy and Emad El-Katori, Europ J Chem 1, 312, (2010).
28. Dr. Rathika. Govindasamy, Swetha Ayappan, J Chil Chem Soc 60, 2786, (2015).
29. Abd El-Aziz S. Fouda, Safaa El-din H. Etaiw, Dina M. Abd El-Aziz and Osama A. Elbaz, Int J Electrochem Sci 12, 5934, (2017).
30. Husnu Gerengia, H. Ibrahim Ugrasb, Moses M. Solomonc, Saviour A. Umorend, Mine Kurtaya and Necip Atare, J Adhes Sci Technol 30, 2383, (2016).
31. Abd El-Aziz S. Fouda, Ali M. El-Azaly, J Bio Tribo Corros 3, 49, (2017).
32. M. Bouanis, M. Tourabi, A. Nyassi, A. Zarrouk, C. Jama, F. Bentiss, Appl Surf Sci 389, 952, (2016).
33. A. S. Fouda, T. Fayed, M. A. Elmorsi, M. Elsayed, J Bio Tribo Corros 3, 1, (2017).
34. J. DAHDELE, I. DANAEE, G.R. RASHED, J Chil Chem Soc 61, 3025, (2016).
35. Y. Zhou, S. Zhang, L. Guo, S. Xu, H. Lu and F. Gao, Studies Int J Electrochem Sci 10, 2072, (2015).
36. Ashish Kumar Singh, Sanjeeve Thakur, Balaram Pani, Eno E. Ebenso, Mumtaz Ahmad Quraishi, and Ajit Kumar Pandey, ACS Omega 3, 4695, (2018).
37. K. R. Ansari, M. A. Quraishi, A. S. Ramkumar and I. B. Obot, RSC Adv 6, 24130, (2016).
38. A. Biswas, S. Pal and G. Udayabhanu, Appl Surf Sci 353, 173, (2015).
39. El Bribri, M. Tabyaoui, B. Tabyaoui, H. El Attari, F. Bentiss, Mat Chem Phys 141, 240, (2013).
40. Abd El-Aziz S. Fouda, Emad E. El-Katori and Saedah Al-Mhyawi, Int J Electrochem Sci 12, 9104, (2017).
41. L. O. Olasunkanmi, I. B. Obot and E. E. Ebenso, RSC Adv 6, 86782, (2016).
42. K. K. Alaneme, Y. S. Daramola, S. J. Olusegun and A. S. Afolabi, Int J Electrochem Sci 10, 3553, (2015).
43. A. S. Fouda, S. A. Abd El-Maksoud and H. M. Mostafa, J Appl Chem 6, 190, (2017).
44. Fouda, M. Ismail, G. EL–ewady and A. Abousalem, J Mol Liq 240, 372, (2017).
45. S. Fouda, A. M. Attiab and A. M. Rashed, Prot Met Phys Chem 53, 743, (2017).
46. Abd El-Aziz S. Fouda, Ahmed A. El-Hossiany, Heba M. Ramadan, Zastita Materijala, 58, 541, (2017).
47. N. Soltani, N. Tavakkoli and M. Ghasemi, Int J Electrochem Sci 11, 8827, (2016).
48. Verma, P. Singh, I. Bahadur, E. E. Eenso, and M. A. Quraishi, J Mol Liq 209, 767, (2015).
49. R. Karthik, P. Muthukrishnan, A. Elangovan, B. Jeyaprabha, and P. Prakash, Adv Civil Eng Mat 3, 413, (2014).
50. M. Pitchaipillai, K. Raj, J. Balasubramanian, and P. Periakaruppan, Inter J Min Metall Mat 21, 1083, (2014).
51. Anees A. Khadom, J Chil Chem Soc 59, 2545, (2014).
52. Ambrish Singh, Mohd Talha, Xihua Xu, Zhipeng Sun, and Yuanhua Lin; ACS Omega 2, 8177, (2017).
53. Wang, M. Du Zhang and J. Gao, Corros Sci 53, 354, (2011).
54. R. Vera, R. Schrebler, P. Cury, R. Del Rio, and H. Romero, J Appl Electrochem 37, 519, (2007).
55. A. Ehsani, M. G. Mahjani, M. Hosseini, R. Safari, R. Moshrefi and H. M. Shiri, J Colloid Interf Sci 490, 444, (2017).
56. A. S. Fouda, A. Emam, R. Refat, M. Nageeb, J Anal Pharm Res 6, 00168, (2017).
57. A. S. Fouda, S. A. Abd El-Maksoud, M. Sh. Zoromba, and A. R. Ibrahim, Int J Corros Scale Inhib 6, 372, (2017). D. Mares, Carlo Romagnoli B. Tosi, Elisa Andreotti, G. Chillemi and F. Poli, 160, 85, (2005).
58. D. Mares, Carlo Romagnoli B. Tosi, Elisa Andreotti, G. Chillemi and F. Poli, 160, 85, (2005).